EFFECT OF VARIOUS EPOXY ON LED ENCAPSULATION PROCESS

DANIEL HAKIMI BIN FAUZAI
J20A0435

A REPORT SUBMITTED IN FULFILMENT OF THE REQUIREMENT FOR THE DEGREE OF BACHELOR OF APPLIED SCIENCE (MATERIALS TECHNOLOGY) WITH HONOURS

FACULTY OF BIOENGINEERING AND TECHNOLOGY

UNIVERSITI MALAYSIA KELANTAN

2024

DECLARATION

I declare that this thesis entitled “Effect of Various Epoxy on Led Encapsulation Process” is the results of my own research except as cited in the references.

Signature :

Student’s Name : Daniel Hakimi Bin Fauzai

Date :

Verified by:

Signature :

Supervisor’s Name : Dr Muhammad Iqbal Bin Ahmad

Stamp :

Date :

ACKNOWLEDGEMENT

In the name of Allah, the most gracious and merciful

Alhamdulillah, first praises to Allah the Almighty for giving me the opportunity and conferring me the ability to complete this study. This thesis cannot be complete without guidance and supervision of several people.

Thousands of appreciations and deepest gratitude to my supervisor, Dr. Muhammad Iqbal Bin Ahmad for his guidance, suggestions, and constant support towards me to producing a good outcome from this study. The completion of this thesis could not have possible without her valuable guidance and persistent help.

I am thankful to University Malaysia Kelantan for giving me chance and opportunity to learning and pursue my study. Moreover, I would also want to show my appreciation to my fyp partners especially Ong Chun Hau for their helps and idea while doing the Ansys Simulation.

Finally, I would like to express my gratitude to my beloved parents, Fauzai Bin Omar and Zauyah Binti Othaman who always give me valuable help and support. To those who indirectly contributed to this research, your kindness means a lot to me. Thank you very much.

Effect of Various Epoxy on Led Encapsulation Process

ABSTRACT

The purpose of this research study is to see the effect of LED Encapsulation on the production of microvoids. The title of this study is the study of LED encapsulation using different types of epoxies. The parameters used to see the effect of microvoids for this study are five different types of epoxies, five different inlet speeds and five different inlet sizes. The method used for the study is the computing method and before making a simulation study it is necessary to confirm with the validation of making a real experiment. The simulation application used is Ansys Fluent, the results from the simulation when completed can see the effect of the resulting microvoid by analysing the data obtained by also looking at the effect of incoming pressure, total fractional volume, and velocity. The results of this simulation can see that this parameter has an effect on the epoxy used on the production of microvoids. It is hoped that this study can provide benefits with the results of this study by analysing the data and identifying ways to minimize the effect of microvoids on LED Encapsulation.

Kesan Pelbagai Epoksi Terhadap Proses Ekapsulasi Led

ABSTRAK

Tujuan kajian penyelidikan ini ialah untuk melihat kesan Pengekapsulan LED terhadap penghasilan mikrovoid. Tajuk bagi kajian ini ialah kajian pengekapulasan LED menggunakan pelbagai jenis epoksi. Parameter yang digunakan untuk melihat kesan mikrovoid bagi kajian ini ialah lima jenis epoksi yang berbeza, lima kelajuan masuk yang berbeza dan lima saiz salur masuk berbeza. Kaedah yang digunakan untuk kajian ialah kaedah pengkomputeraan dan sebelum membuat kajian simulasi perlu mengesahkan dengan validasi membuat eksperiment yang sebenar. Aplikasi simulasi yang digunakan ialah Ansys Fluent, keputusan daripada simulasi apabila telah selesai dapat melihat kesan mikrovoid yang terhasil dengan menganalisis data yang diperoleh dengan melihat juga kesan daripada tekanan yang masuk, jumlah isipadu pecahan dan halaju. Hasil daripada simulasi ini dapat melihat bagi parameter ini memberikan kesan kepada epoksi yang digunakan terhadap penghasilan mikrovoid. Dengan ini mengharap kajian ini dapat memberikan manfaat dengan hasil daripada kajian ini dengan menganalisis data dan mengenal pasti cara untuk meminimalkan kesan mikrovoid terhadap Pengekapsulan LED.

TABLE OF CONTENT

LIST OF FIGURES

LIST OF TABLES

LIST OF ABBREVIATION

EMC	Epoxy Moulding Compound
CFD	Computational fluid dynamics
Kg/m^3	Kilogram per cubic metre
Kg/m. s	Kilogram-meter per second
N/m	Newton-meter
Mm	Millimetre
S	Second

LIST OF SYMBOLS

®	registered trademark ownership

CHAPTER 1

INTRODUCTION

1.1 Background of Study

The phenomenon known as microvoids results from the LED encapsulation process, where small air bubbles or voids are formed within the material of the LED chip. The primary purpose of LED chip encapsulation is to safeguard against environmental contaminants, and utilizing materials like transparent epoxy enhances the LED's longevity. The presence of microvoids, often ranging from a few micrometres to several millimetres in size, is attributed to factors such as uneven mixing conditions, incomplete mold filling, and inadequate encapsulation mixing.

Moreover, the durability and lifespan of LEDs are intricately linked to the occurrence of microvoids. These minute open spaces create avenues for dirt and moisture ingress, leading to corrosion and potential damage to the LED chip. Additionally, fluctuations in temperature cause the trapped air within the voids to contract, exerting pressure on the material covering the LED chip. Ensuring durability and adherence to set standards becomes crucial in mitigating these effects.

LED encapsulation finds widespread application across diverse industries, including automotive, housing, medicine, and electronic equipment. In the automotive sector, the emphasis on energy efficiency, extended lifespan, and enhanced brightness underscores the significance of effective LED encapsulation. The reliability of LED products is paramount in ensuring safety and increasing investment potential within the industry. Innovation continues to drive advancements in LED technology, particularly in fields like medicine, where patient

safety is a top priority. Rigorous processing of LEDs for applications in operating rooms is essential to eliminate health risks associated with lead exposure.

In this study, a comprehensive examination of LED encapsulation is conducted through a systematic approach. The research involves an experiment employing verification processes prior to simulations, utilizing drawings and computational methods in two dimensions. Specifically, ANSYS Fluent is employed as the application for creating sketches and running simulations to analyse and extract relevant data. The focus is on comparing five different types of epoxies, each with distinct concentrations and viscosities, to identify the epoxy with the least microvoid production effect. This experimental design aims to contribute valuable insights to the optimization of LED encapsulation processes for improved performance and reliability.

1.2 Problem statement

The investigation into LED encapsulation presents a distinct challenge when transitioning from the physical experiment to computational simulations, employing the Computational Fluid Dynamics (CFD) method. The central issue revolves around replicating the real-world dynamics of epoxy flow from the inlet to the LED within the simulation environment. Achieving this emulation necessitates a thorough study and precise referencing to establish optimal simulation settings mirroring the conditions of the actual experiment.

One critical aspect to address is the behaviour of the epoxy as it descends from the inlet onto the LED surface. Ensuring that the simulated epoxy flow accurately mirrors the physical experiment requires meticulous attention to detail and a nuanced understanding of the fluid dynamics involved. Achieving an authentic representation of the experiment in the simulation involves defining parameters such as viscosity, gravity, and fluid interaction forces with precision.

Furthermore, the challenge extends to the manipulation of wind pressure settings within the simulation. Fine-tuning the velocity of the epoxy is crucial for capturing the nuanced aspects of its descent onto the LED. As the velocity decreases, factors such as turbulence and the impact of gravity become more pronounced, requiring a delicate balance in setting wind pressures to achieve a realistic simulation outcome.

The number of meshes used in the simulation poses an additional hurdle. Striking the right balance between computational efficiency and accuracy is paramount. A thorough examination of mesh resolution is required to ensure that the simulation captures the intricate details of epoxy flow while maintaining computational feasibility.

In summary, the problem at hand involves bridging the gap between the physical LED encapsulation experiment and its computational counterpart. This necessitates a comprehensive understanding of fluid dynamics, precise parameterization, and the optimization of simulation settings, particularly in managing wind pressures and mesh considerations. Addressing these challenges will contribute to the successful implementation of the simulation, providing valuable insights into the intricacies of LED encapsulation processes.

1.3 Expected Outcomes

The primary objective of this research is to scrutinize the encapsulation process by conducting a detailed analysis of microvoid effects through Computational Fluid Dynamics (CFD) simulations. The ultimate goal is to derive conclusive results from these simulations, allowing for a discerning examination of variations in pressure, total fractional volume, and velocity. This analysis will be carried out across three key parameters: five different epoxy types, five distinct input speeds, and five varied input sizes.

By systematically investigating these parameters, the research aims to unveil disparities in the microvoid effects generated during the encapsulation process. This

comprehensive exploration will facilitate the identification and understanding of factors influencing the production of microvoids, ranging from minimal to substantial quantities.

Anticipated outcomes of this research include a nuanced comprehension of how different epoxy types, input speeds, and input sizes impact microvoid formation during LED encapsulation. The findings are expected to shed light on variations in pressure dynamics, fractional volume distribution, and velocity patterns under diverse experimental conditions.

Ultimately, the results of this research aspire to provide valuable insights into optimizing the LED encapsulation process. By elucidating the effects of different parameters on microvoid formation, the study aims to contribute knowledge that can be leveraged for enhanced LED manufacturing practices. The identification of optimal conditions and materials has the potential to improve the quality and reliability of LED products, thereby benefiting industries reliant on efficient and durable LED technology.

1.4 Objectives

1) To validate the epoxy in simulation.
2) To investigate the microvoid effect of epoxy on LED encapsulation prosses by looking at the volume of fraction, pressure, and velocity.

1.5 Scope of Study

The scope of this study is to investigate the effect of microvoids from the LED encapsulation process by using Computational Fluid Dynamics (CFD) simulations. By using three different parameters for analysis, namely five different types of epoxies, five different types of input speed, and five different types of input sizes. Furthermore, with the data obtained, it is possible to see the difference in the resulting velocity, quantity of volume of fraction and

pressure produced when performing different analyses. It can see what affects the increase of the microvoid effect on the encapsulation process on the three parameters and this can give a conclusion on the parameters used which parameters and analysis have the least microvoid effect on the encapsulation process.

1.6 Significances of study

The importance of investigating the effect of microvoid on the encapsulation process is that the analysis carried out can help find out what the effect is using different parameters, and the verification carried out between the experiment and the simulation can be seen as to what percentage of similarities there are between the two using the same settings as the experiment made in the simulation. Furthermore, by using simulation, you can see many more analyses obtained because by using Computational Fluid Dynamics (CFD) simulations, you can see results such as pressure produced, volume of fraction, density, velocity and many more. With the use of simulation, it is possible to repeat the simulation if it fails to achieve the desired objective and make the simulation until it obtains the desired result without incurring high costs.

CHAPTER 2

LITERATURE REVIEW

2.1 Encapsulation in the chemical industry

Encapsulation of active ingredients is a prominent area of focus in both academic and industrial research, playing a pivotal role in enhancing the efficiency, stability, compatibility, safety, and targeted delivery of these ingredients. Through the synthesis process, the encapsulation of active ingredients leads to improved formulations, new market access, product differentiation, increased compatibility, and stability, thus meeting consumer demands with superior performance and reduced costs. Key areas of emphasis within the industry include supramolecular encapsulation, aqueous self-assembly systems, and emulsion-based capsules.(Andrade et al., 2015)

In the realm of supramolecular encapsulation, small molecules are included in structural cavities, utilizing entropically weak intermolecular interactions and enthalpy-favorable effects to release solvents from molecular compartments. This approach, rooted in supramolecular chemistry, finds applications in diverse industries such as food, pharmaceuticals, and chemicals.

Vesicle encapsulation, on the other hand, involves a self-assembly process where molecules are wrapped in high-level structures, forming bilayer membranes with a closed aqueous core. Utilizing stabilizers in aqueous systems, vesicles serve as a structural motif for encapsulation and are employed in various industries, particularly in encapsulating protective substances for active ingredients.

Emulsion encapsulation, a widely used method in fields like coating, microbial control, agrochemistry, food, and nutrition, involves the formation of robust wall-shells. This

process consists of emulsion formation followed by fabrication with a separation barrier, facilitating the creation of ordered microscale and macroscale structures.

A critical aspect of encapsulation lies in achieving stabilization, delivery, isolation, and controlled release of active ingredients from particles or capsules. As the encapsulation process evolves through product synthesis, improvements in efficiency, compatibility, safety, and other factors contribute to the overall advancement of the industry. Liquid products, often featuring complex combinations of solvents, surfactants, buffers, defoamers, fragrances, and additives, demand effective packaging materials with barriers to maintain stability amid non-uniform formulations.

In conclusion, the diversity of formulations enhances performance and introduces new technologies. Robust stability offered by encapsulation mitigates the impact of various formulation additives, fostering a stable and sustainable industry. This advancement contributes to increased user safety, cost savings, and optimized chemical usage across diverse fields, solidifying encapsulation's role in creating a resilient industry for the future.

2.2 LED market industry

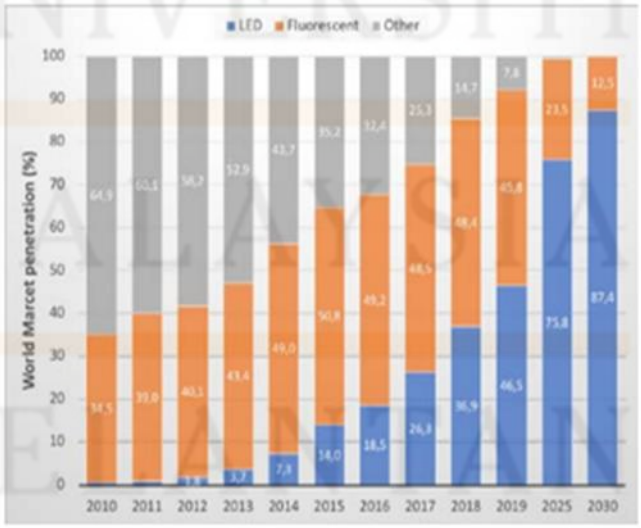

Figure 2.1: Penetration Rate of LED, Reflected in Sales, Demonstrates Rapid Growth: Insights from IEA Data [IEA-19](Zissis, G., Bertoldi, P., Serrenho, 2018)

The burgeoning adoption of LEDs in indoor lighting, as illustrated in Figure 2.1, reflects a notable shift, surpassing fluorescent lamps in sales due to the cost-effectiveness of LED manufacturing. The global LED usage witnessed a substantial surge, marking a 5% increase in 2013, and by 2019, half of the global lighting sales were attributed to LEDs, particularly integrated LED luminaires. To align with Sustainable Development Goals (SDS), projections indicate that LEDs must constitute over 90% of product sales by 2030.

The prominence of the global lighting market, encompassing both lamps and luminaires, is underscored by a significant market share. Approximately 75% of the global lighting market emanates from luminaires/fixtures, with the remaining 25% attributed to lamps. Figure 2.0 vividly portrays the substantial market expansion, buoyed by robust growth in global infrastructure activities.

The reduction in LED prices, culminating in a cumulative $38 billion in sales for LED lighting products over the past five years, has intensified competition among standard LED manufacturers. This affordability, coupled with continuous innovation, empowers customers with diverse product choices at reasonable prices.

This competitive landscape has far-reaching implications, propelling LED utilization across various applications, including residential, commercial, and architectural lighting. The economic advantages extend beyond initial affordability, encompassing long-term savings through reduced lamp replacements in newly constructed buildings. Both private enterprises and governmental bodies can institute maintenance measures in existing residential, cloud, and commercial structures, further reinforcing the market dynamics. In conclusion, the LED

industry stands poised for a radiant future, driven by competitive pricing and a spectrum of innovations. These factors collectively contribute to the industry's enduring.

2.2.1 Commercial lightning in LED encapsulation industry

The LED encapsulation industry has become an essential part of the commercial lighting sector due to its ability to enhance the durability and performance of LED chips. LED encapsulation involves enclosing the LED chips in a protective material that can withstand harsh environmental conditions and increase their lifespan. As a result, the encapsulation process has become a popular choice for manufacturers looking to produce energy-efficient and long-lasting lighting solutions for commercial and residential applications.

Figure 2.2: Commercial lightning product(*Silicone Encapsulation – TIC Industries*, n.d.)

In figure 2.2 show the example product that the commercial lighting sector has been a major driver of this growth, with businesses and organizations looking to reduce their energy consumption and operating costs. LED encapsulation has become a critical component of commercial lighting as it enables manufacturers to produce high-quality and long-lasting lighting products that can withstand the harsh conditions of commercial environments. As the industry continues to innovate and develop new encapsulation techniques and materials, the

commercial lighting sector is expected to continue its strong growth trajectory, providing businesses with innovative and cost-effective lighting solutions.

2.2.2 Automotive in LED encapsulation industry

The automotive industry has also been a significant player in the LED encapsulation industry. LED lights have replaced traditional halogen bulbs in many automotive applications, including headlights, taillights, and interior lighting. This shift has been driven by the many benefits that LED lights offer, such as increased energy efficiency, longer lifespan, and brighter illumination. In addition to these benefits, LED lights also allow for more flexible and innovative designs, which has been a major draw for automakers looking to differentiate themselves in a crowded market.

Figure 2.3: High-Power Led encapsulation inspection (*High-Power LED Encapsulation Inspection – Electronics | Cognex,* n.d.)

For figure 2.3 inspection proses to meet the specific needs of the automotive industry, LED encapsulation materials must meet strict requirements for durability, reliability, and safety. This has led to the development of specialized materials and encapsulation techniques that can withstand the harsh conditions of the automotive environment, such as extreme temperatures, vibration, and moisture. As the adoption of LED lighting in the automotive

industry continues to grow, the LED encapsulation industry is expected to see continued investment and innovation in this area.

2.3 Light-Emitting Diode (LED) encapsulation material

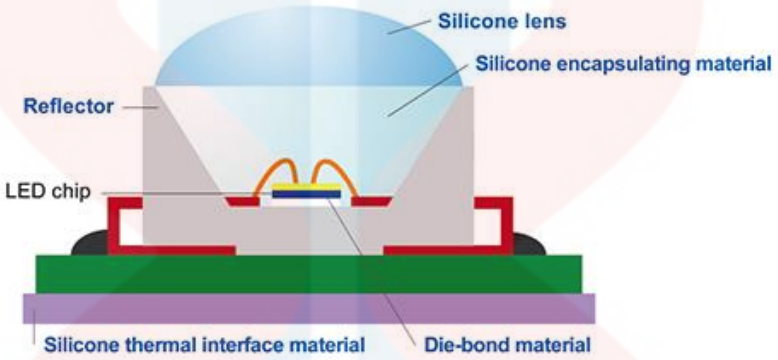

Figure 2.4: The structure of a LED (*Shin-Etsu Silicone : Silicone Materials for LEDs*, n.d.)

In figure 2.4 show structure of LED encapsulation and for process of protecting and enclosing a light-emitting diode (LED) chip using a material that enhances its performance and protects it from environmental factors. The encapsulation process is critical in determining the lifespan, brightness, and reliability of LED products. Encapsulation materials must have good thermal conductivity, mechanical strength, chemical resistance, and optical properties to ensure optimal LED performance.

Environmental conditions also play a crucial role in LED encapsulation. Exposure to moisture, heat, and UV light can cause degradation and failure of the encapsulation material, leading to reduced LED lifespan and performance. Manufacturers must carefully control the encapsulation process, including the curing time, temperature, and humidity, to ensure optimal performance and reliability. In addition, the use of lead-based encapsulation materials has become a concern due to the potential environmental and health risks associated with lead

exposure. As a result, there is a growing need for alternative, eco-friendly encapsulation materials that can provide the same level of performance without the environmental and health risks.

2.4 Microvoid

Microvoids are a common issue in the encapsulation of LEDs. These are tiny gas-filled cavities that can form within the encapsulant during manufacturing. Microvoids can have a significant impact on the performance and reliability of LEDs. When light passes through the encapsulant, it can be scattered by the microvoids, leading to reduced luminous efficiency and colour shift. Additionally, microvoids can create areas of high stress within the encapsulant, leading to premature failure of the LED.

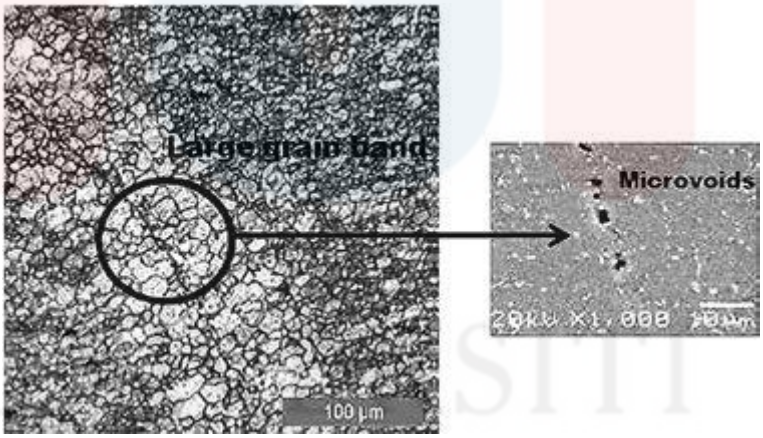

Figure 2.5: Example of Microvoids (Çevik et al., 2016)

In figure 2.5 show microvoid, this mitigate microvoid formation, manufacturers must carefully control the encapsulation process. This can involve controlling the temperature and pressure of the encapsulant and the rate of curing. Additionally, manufacturers may use additives to the encapsulant to reduce the formation of microvoids. By carefully managing the encapsulation process, manufacturers can reduce the incidence of microvoids and improve the

performance and reliability of their LEDs. The relatively high toughness observed for the rubbers which possessed not chemically reactive, functional end groups raises the question of how an epoxy polymer simply containing holes, or voids, would behave. (Y. Huang & Kinloch, 1992)

2.5 Computer-Aided Design (CAD)

The conceptual design phase serves as the initial stage in the development of the program airframe. During this phase, a comprehensive design concept is formulated, employing detailed computer-aided drafting (CAD). Initial ideas are often conveyed through napkin sketches, and the integration of realistic CAD facilitates a potentially effective approach. This amalgamation of technology and artistic capabilities allows engineers to input various parameters and swiftly model ideas. Efficient conceptual design not only explores a multitude of concept ideas but also saves valuable time, particularly crucial in industries like aerospace where time is synonymous with money.(Ley 25.632, 2002)

The advanced CAD model produced during this phase aims to provide initial weights with estimates, assess structural integrity, and define shapes with unique characteristics. The enhanced model offers designers the flexibility to modify features such as windows, exits, cabin pressure, and other fundamental airframe structures promptly. This capability proves beneficial for both employees and the marketing team, as alterations or additions can be implemented swiftly, and the CAD program provides immediate feedback on the impact of the design changes. Moreover, the detailed design phase involves modelling the structure in a CAD program and exporting it to Finite Element Analysis (FEA) allows engineers to identify stress hotspots and potential weaknesses in the conceptual design.

In a related experiment involving the use of Ansys Software, the objective is to draw an LED based on provided measurements. An LED, or Light Emitting Diode, functions as a

semiconductor device emitting light when an electric current is applied. When utilizing Ansys software for drawing an LED, it is imperative to include essential components such as anode and cathode pins, the LED housing or package, and the light-directing lens. Ansys Software ensures precise and accurate design of these components, guaranteeing optimal performance of the LED. Additionally, the software enables simulation of the LED's behaviour under diverse conditions, facilitating further optimization of the design. In summary, Ansys software emerges as an excellent tool for the meticulous design and simulation of LEDs across a broad spectrum of applications.

2.6 Epoxy Resin

Epoxy resins constitute a significant class of polymers characterized by the presence of multiple three-membered rings, commonly referred to as epoxy, epoxide, oxirane, or ethoxyline groups. Precisely defined, the term "epoxy resin" pertains to uncrosslinked monomers or oligomers containing epoxy groups. Additionally, this term is loosely used to encompass cured epoxy systems, characterized by a very high molecular weight, and containing minimal or no epoxide groups. These resins are predominantly dual or multi-functional epoxides, finding applications across diverse industries.(Ham et al., 2012)

Monofunctional epoxides serve various purposes in the realm of polymers, functioning as reactive solvents, viscosity modifiers, or adhesion promoters. Epoxy, as a versatile class, finds application in diverse fields such as tin coating for metals, automotive primers, printed circuit boards, semiconductor encapsulation, adhesives, and aerospace composites. Epoxy is particularly known for imparting amorphous thermoset properties with exceptional mechanical strength, toughness, chemical resistance, moisture and corrosion resistance, as well as good thermal, adhesive, and electrical properties. Its unique combination

of properties, including negligible volatile emissions, low shrinkage, and dimensional stability, sets epoxy apart from other plastics.

Furthermore, the outstanding performance features of epoxy resins can be enhanced through formulation, making them a versatile and cost-effective choice for structural bonds and protective coatings. Commercial epoxy resins exhibit aliphatic, cycloaliphatic, or aromatic backbones and are available in a range of molecular weights. They react with a diverse array of curing agents across various temperature conditions, providing additional flexibility in their application. The wide acceptance of epoxy resins as a material of choice for structural bonding and protective coatings can be attributed to their superior performance characteristics and versatility at a reasonable cost.

The five types of epoxies used for this investigation are among the many epoxy resins appropriate for LED encapsulation. The selection of epoxy is influenced by several factors, including the micro voids, application's requirements, temperature stability, optical properties, and production processes. The following epoxy resins that will be use in this investigation for LED encapsulation:

1. Epoxy Molding Compound (EMC): providing a durable and stable protective layer through its thermosetting properties. This encapsulation safeguards LEDs from environmental factors and mechanisms. EMC's efficient thermal conductivity supports heat dissipation, factor for optimal LED performance. EMC's compatibility with semiconductor materials and its versatility in colours and transparency further contribute to its significant in LED packaging.

2. D.E.R.-331: As a versatile and high-performance material, D.E.R-331 is known for its excellent adhesion, thermal stability, and resistance to chemicals. This epoxy resin often employed as a binder in the formulation of coatings, adhesives, and composite materials. With a well-balanced combination of mechanical strength and flexibility, D.E.R.-331 contributes to the durability and performance of the product.

3. ERL-4221: Cycloaliphatic, diepoxy functional organic compound, serving as a valuable foundation component in the synthesis of epoxy resins with semi-hard to hard curing characteristics, well- suited for elevated temperature applications. This versatile compound finds applications in casting resins, reinforced plastics, and solvent-free adhesives systems, offering UV resistance and anti-radiation properties.

4. Master Bond EP30-2: Applications were maintaining the transparency of encapsulant is crucial for efficient light transmission. The rapid curing time, provides flexibility in manufacturing processes, allowing for efficient. Its resistance to water, chemical and extreme temperature with demand conditions. Master Bond EP30-2 stands out as reliable solution for LED encapsulation, meeting both performance and processing requirements.

5. Epotek OG198-54: its low viscosity and simple ten-to-one mix ratio facilitate easy processing in manufacturing. This epoxy's exceptional optical clarity enhances light transmission in LED applications, while its robust physical strength and resistance to environmental factors ensure durability. With dimensional stability and success in cryogenic applications.

2.7 Computational Fluid Dynamics (CFD) Analysis

Research functions as a mechanism for understanding the behavior of physical phenomena, including fluid flow, heat and mass transfer, and chemical reactions, as evidenced throughout history. This pursuit has been traditionally categorized into two fundamental types: theoretical and purely experimental. The advent of computing technology has introduced a third category of equal significance in fluid dynamics known as computational fluid dynamics (CFD). This computational approach is a potent tool, enabling scientists to conduct numerical experiments within a virtual laboratory. The widespread utilization of CFD spans various industries, encompassing the automobile sector, architecture, health, and chemical processes. CFD offers

a cost-effective alternative to traditional experimental setups, allowing scientists to explore fluid flow phenomena comprehensively without requiring expensive physical rigs. While real-world experiments typically provide observations of desired parameters, CFD offers the advantage of generating data with exceptional resolution. Operating as software, CFD is adaptable to any computer and can be accessed by multiple users, presenting a versatile and accessible solution. The distinct advantage of CFD lies in its ability to replace real-world experiments, resulting in significant cost savings. (Visualization, 2020)

In the LED encapsulation industry context, the use of Ansys® CFD analysis proves indispensable. LED encapsulation involves carefully sealing LED components within a protective package to mitigate damage from external elements. Ansys® CFD analysis is crucial in optimizing the encapsulation process by simulating fluid flow behavior and offering a detailed analysis of the package's thermal characteristics. This analytical tool empowers engineers to make informed decisions regarding package design, ensuring the adequate protection of LED components while optimizing thermal performance.

Furthermore, Ansys® CFD analysis extends its benefits to designing and developing LED lights for commercial, automotive, and consumer electronics applications. Engineers leverage this tool to simulate fluid flow behavior in LED fixtures, thoroughly analyze the system's thermal performance, and make informed design decisions to enhance overall efficiency. Ansys® CFD analysis becomes instrumental in optimizing the design of LED fixtures, contributing to reduced energy consumption, improved heat dissipation, and increased LED component lifespan. This tool proves essential in the LED encapsulation industry, assisting engineers in crafting innovative LED lighting solutions that align with the rigorous requirements of diverse industries.

CHAPTER 3

MATERIALS AND METHODS

3.1 Introduction

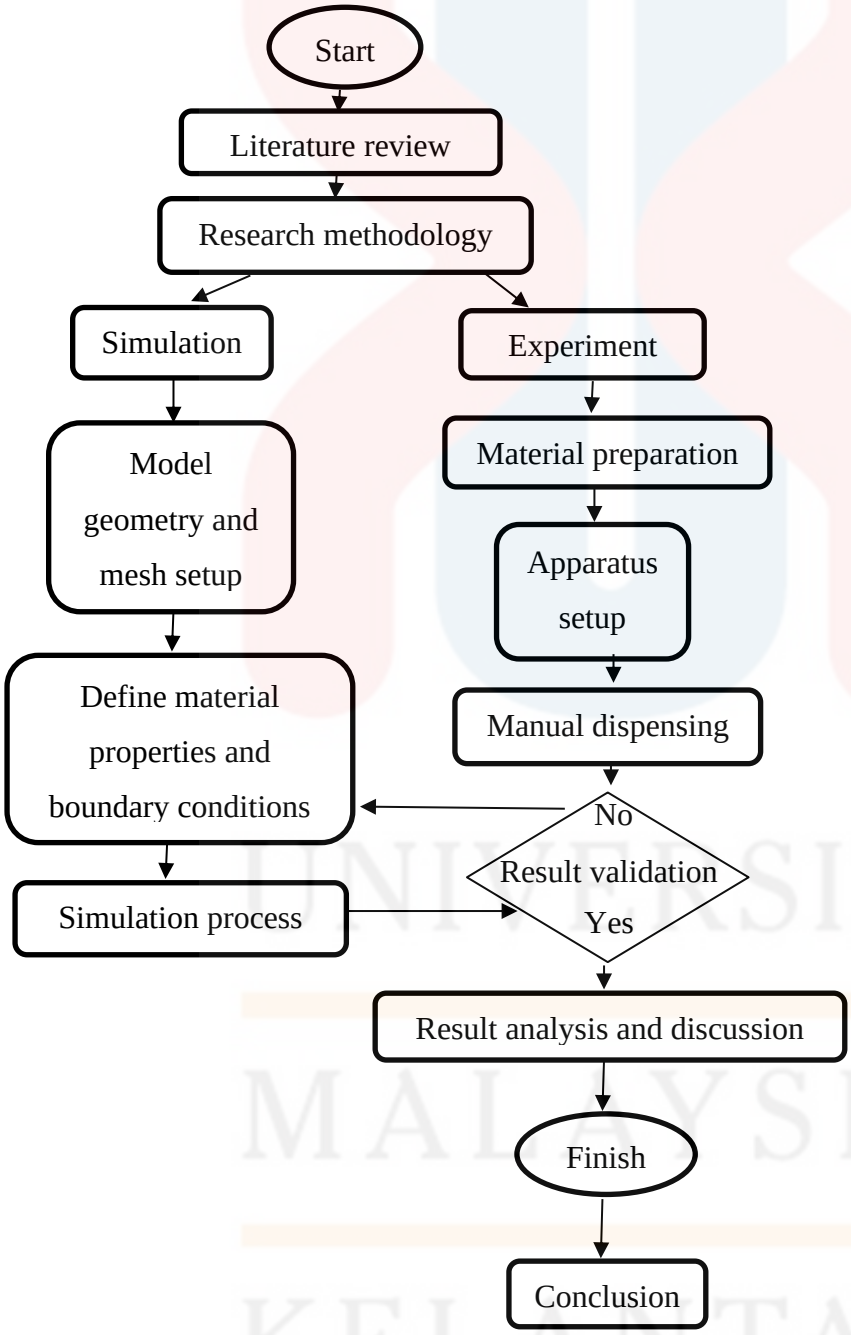

Figure 3.1: Research Flow Chart

In this chapter, two things are stated: the materials used and the methodology. The materials used for this research are briefly explained in the first part. There are two parameters used in this chapter. The first is the material used, which is the LEDs that are used with the actual size of the LEDs to be sketched, and the second parameter is the use of epoxy to be used in this simulation in Ansys Software. The results collected from the simulation analysis were compared between the parameters with the difference of epoxy used for this simulation.

3.2 Governing Equation

The governing equations of fluid dynamics are the continuity, momentum, and energy equations (Anderson, 1992). These equations describe the behaviour of fluids in motion and are conventionally obtained from rigorous first principles such as the conservation laws or knowledge-based (Chen et al., 2021). This method involves using a library of candidate functions and sparse regression to identify the important terms in the governing equations. The objective is to find the closed form of the equations from incomplete, scarce, and noisy spatiotemporal measurements.

Newtonian fluids, and conservation of energy equation. These equations are expressed as follows:

Continuity (conservation of mass) equation (Rapp, 2022):

$$\partial u/\partial x + \partial v/\partial y + \partial w/\partial z = 0 \quad (1)$$

where u, v and w are velocities of the fluid that flow in x, y, and z axis respectively.

The Navier-Stokes equation for x-direction:

$\partial u/\partial t + u\ \partial u/\partial x + v\ \partial u/\partial y + w\ \partial u/\partial z = -1/\rho\ \partial P/\partial x + [\ \partial/\partial x\ (\eta\ \partial u/\partial x) + \partial/\partial y\ (\eta\ \partial u/\partial y) + \partial/\partial z\ (\eta\ \partial u/\partial z)] + gx$ (2)

The Navier-Stokes equation for y-direction:

$\partial v/\partial t + u\ \partial v/\partial x + v\ \partial v/\partial y + w\ \partial v/\partial z = -1/\rho\ \partial P/\partial y + [\ \partial/\partial x\ (\eta\ \partial v/\partial x) + \partial/\partial y\ (\eta\ \partial v/\partial y) + \partial/\partial z\ (\eta\ \partial v/\partial z)] + gy$ (3)

The Navier-Stokes equation for z-direction:

$\partial w/\partial t + u\ \partial w/\partial x + v\ \partial w/\partial y + w\ \partial w/\partial z = -1/\rho\ \partial P/\partial z + [\ \partial/\partial x\ (\eta\ \partial w/\partial x) + \partial/\partial y\ (\eta\ \partial w/\partial y) + \partial/\partial z\ (\eta\ \partial w/\partial z)] + gz$ (4)

were

ρ = density

u = velocity vector in x-direction

v = velocity vector in y-direction

w = velocity vector in z-direction

P = static pressure

t = time

η = viscosity

gx, gy and gw = gravity in x, y and z-axis

The epoxy viscosity is assumed to be constant at high temperature. So, the Newtonian fluid equation (Yahia et al., 2016):

$\eta = \tau/\gamma$ (5)

were

τ = shear stress

γ = strain

The governing equation for surface tension often described by the Young-Laplace equation, which relates the pressure difference across a curved liquid interface to the surface tension and the curvature of the interface. The equation is as follows(Bush & John, 2010):

$$\Delta = \frac{2 \cdot \gamma}{R}$$

Where:

ΔP is the pressure difference across the interface.

γ is the surface tension of the liquid

R is the radius of curvature of the liquid interface.

This equation is derived from the balance of forces acting on the liquid interface and is fundamental in understanding the behavior of liquid surfaces and droplets.

3.3 Simulation Modelling

This process starts with measuring the size of the actual LED to get the exact size of the actual LED to use, followed by rounding the body of the LEDs. Figure 3.2 clearly shows the process of designing LEDs using Ansys Software. The dimensions of the LEDs and inlet are determined as follows in Table 3.1.

Table 3.1: Dimensions of LEDs and inlet

No	Specification	Value
1	LEDs width (mm)	1.18
2	LEDs surface diameter (mm)	4.2
3	LEDs bottom diameter (mm)	2.34
4	Distance LEDs to syringe (mm)	10
5	inlet width (mm)	1.8
6	inlet diameter (mm)	3
7	Small LEDs diameter (mm)	0.15
8	Small LEDs width (mm)	0.1

LEDs and Syringe designed in 2D, and it follow the actual size, but the syringe size been modified to meet the requirements to epoxy drop like real simulation because of the setting. The simulation will make LEDs coated with epoxy droplets, allowing them to spread freely. The contact angles of the droplets were measured instantly using a contact angle meter called DIGIDROP while they were in this free-spreading state.(Zhang & Lee, 2012)

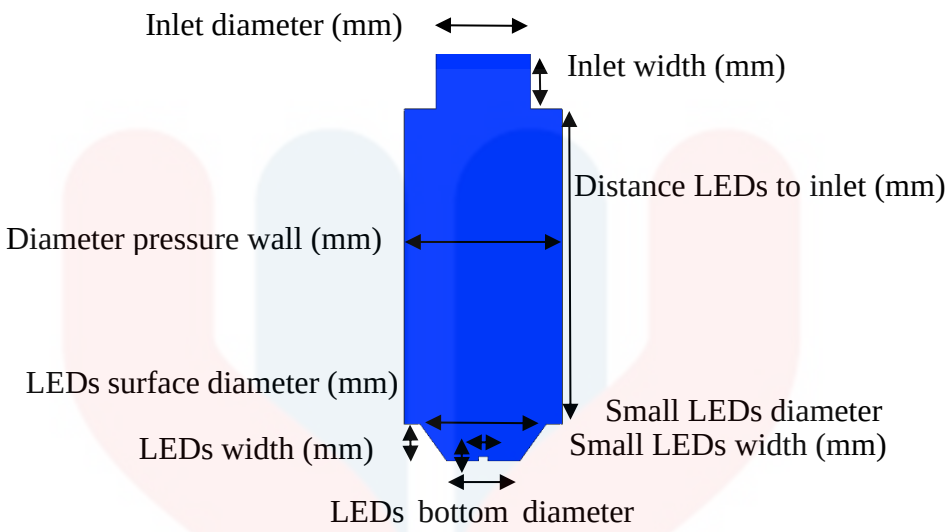

Figure 3.2: Precision scaled model design: reflecting actual dimensions

Figure 3.2 shows the design of LEDs according to the size measured from the actual LEDs like the Figure 3.4. This design is also specific in making the following process for the LEDs encapsulation process by placing Epoxy on top of the LEDs by using Syringe to looking different Epoxy effect at the LEDs surface and what results can be obtained from the encapsulation process. The formation and breakage of bubbles occur when a hemispherical thin sheet reaches a certain thickness, resulting in the production of small droplets. The quantity and dimensions of the droplets are influenced by multiple factors such as the size of the bubble, surface tension between air and liquid, viscosity of liquid, and thickness of the bubble sheet. However, the researchers only witnessed one instance of bubble formation and breakage during their observation (Ribeiro et al., 2023).

3.4 Material Properties and Boundary Condition

Table 3.2: Material properties for five different epoxies

Material	**E1**	**E2**	**E3**	**E4**	**E5**
Properties	Epoxy Molding Compound (Roslan et al., 2020)	ERL-4221 (J. C. Huang et al., 2004)	D.E.R.-331 (J. C. Huang et al., 2004)	Epotek OG198-54 (*EPO-TEK ® OG198-54*, n.d.)	Master Bond EP30-2 (*EP30-2 Product Information | MasterBond.Com*, n.d.)
Density (kg/m^3)	1800	1173	1159	1170	1050
Viscosity (kg/m. s)	0.448	0.224	0.896	0.015	0.04
Surface Tension (N/m)	22	22	22	22	22

Table 3.3: Boundary Condition

Boundary Condition	**Detail**
Inlet speed (m/s)	0.33
Injection Time (s)	1e-6
Inlet Contact Angle (degree)	10
LED contact Angle (degree)	117
Distance needle to base (mm)	11.18

Base Diameter (mm)	2.3

3.5 Experiment Setup

The purpose of the LED encapsulation is to compare the simulation's output to actual results to validate it. A 10 ml syringe, an 8G flat head needle with a 0.8mm-diameter tip, an LED 5050 chip, and epoxy glue are required for the experiment.

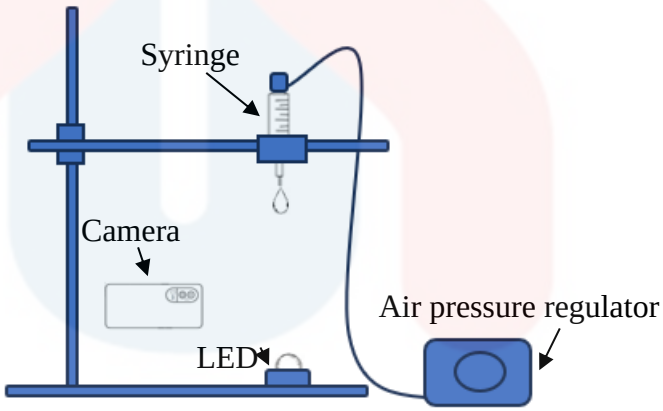

Figure 3.3: Illustration for experiment setup

As for figure 3.3, it shows the experiment setup that has been done using several equipment such as retort stand, syringe, LED 5050, air pressure regulator and smartphone camera. The distance between the syringe and the LED is 10 mm measured using a ruler. By using the smartphone camera to record using slow motion video to be able to see more clearly the effects of epoxy falling on the LED. The first step that has been made is to organize according to figure 3.3. after that, put the epoxy molding compound in the syringe and cover it

with the air pump head and put the LED under the syringe and press the air pump at the right rate and start recording the video using the smartphone camera after that see the results of the experiment if it is according to what is required if not repeat the step of pressing the air pump again until get the desired result.

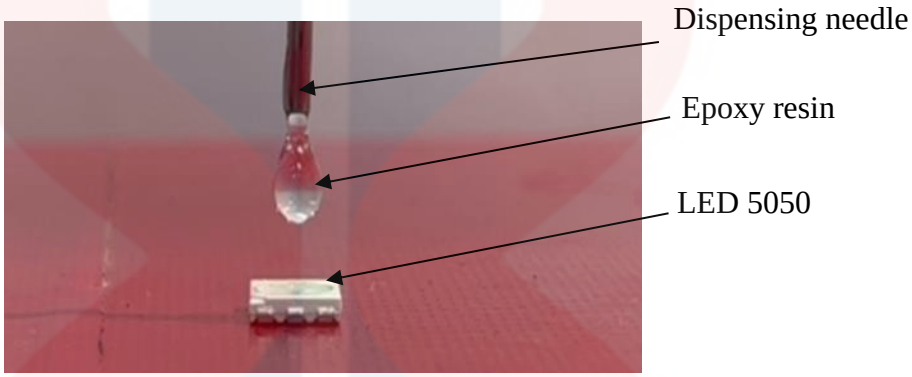

Figure 3.4: Close-up view of epoxy resin simulation setup

As the experiment is being carried out, pictures are being captured to be imported into ImageJ for analysis. The simulation results acquired using ANSYS software will be validated using the results from ImageJ's research. The LED 5050 chip is first set onto a level surface. Then, epoxy resin is injected into the syringe and onto the LED surface. The fluid can take on a hemispheric shape thanks to the mould cavity of the LED substrate. The fluid dispensing procedure is captured on camera using ImageJ software, and the results are analysed. The experiment results are then contrasted to those from simulations using the ANSYS program.

CHAPTER 4

RESULTS AND DISCUSSION

4.1 Overview

This chapter were discussed about both on the experimental and simulation results obtained from the study. The influence of different epoxy resins and micro void on the epoxy resin on the LED during the encapsulation process will be analysed and studied. The structure the epoxy resins obtained during the simulation and experimental is compared for the results validation. There are three parameters that will be analysed which are the total deformation, micro void on LED when epoxy resin drop. The trend of these parameters will be obtained by varying the manipulation variables, different epoxy materials and effect of microvoid.

4.2 Grid Independent Test

For computational fluid dynamics (CFD) solver to generate a proper solution, a quality mesh with optimum number of nodes and elements is needed (Chirica et al., 2019). To choose the appropriate mesh element size for the simulation analysis, five models with different element size are examined: Mesh-1, Mesh-2, Mesh-3, Mesh-4, and Mesh-5. EMC is used to perform the grid independent test for the different mesh size as illustrated in Figure 4.1. Table 4.1 shows the statistic of mesh elements and computational time for each model used in the grid independent test.

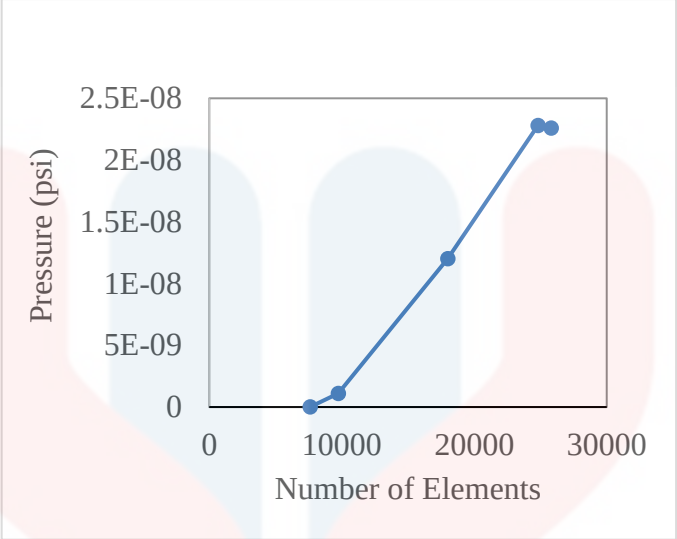

Figure 4.1: Pressure (psi) trends in relation to element quantity

Table 4.1: Statistic of mesh elements and computational time

Mesh type	Nodes	Elements	Computational times (hr)
Mesh-1	26418	25796	14
Mesh-2	25432	24816	12
Mesh-3	24446	18000	10
Mesh-4	10098	9722	8
Mesh-5	7944	7600	6

Based on the result in Figure 4.1, the pressure against Number of Elements used as variable to make the comparison between each mesh type. The value for Mesh-4 and Mesh-5 are due to inaccurate to and low-quality mesh of quality. Figure 4.1 shows the mesh error in mesh-4 and 5. The mesh error occurred due to the large element size which is compatible with the model thus eliminating both mesh-4 and 5 from the selection. For Mesh-1 with 26418 nodes

and 25796 elements, the pressure value is 0.0000226 MPa. Besides, Mesh-2 with 25432 nodes and 24816 elements, the pressure value is 0.0000228 MPa. Next, the percentage difference between both reading is only 0.8% which is less than 1%. Moreover, Mesh-3 with 24446 nodes and 18000 elements with percentage difference of 38.51%.

For the simulation part, the selection of the mesh type and size based on the complexity, convergence, accuracy requirements and computational time required to solve the calculation for 1e-6 times step size. From the results of grid independent test, Mesh-2 with 0.049 mm element size is selected as the standard for the simulation in this study. This is because it can generate the similar result with minimal percentage error which less than 0.8 % compared to Mesh-3 with 38.51 %. Furthermore, the higher the number of cells, the higher the computation power of the computer is required. The computational time recorded Mesh-2 is 12 hours. To conclude, Mesh-2 with element size 0.049 mm is chosen as it can save more energy and computing time.

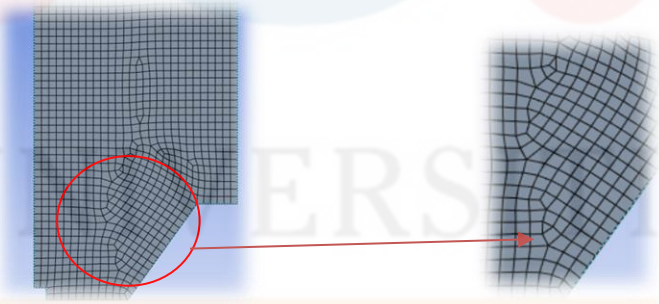

Figure 4.2: Skewness distribution in Ansys meshing

4.3 Validation of Simulation and Experimental Methods

In this section, the simulation result of the encapsulant structure using Ansys results is compared with the experimental for 1 epoxy resin to validation. Both fluids have the same viscosity. Figure 4.3 shows the simulation results for the EMC and Table 4.2 shows the comparison between simulation and experimental.

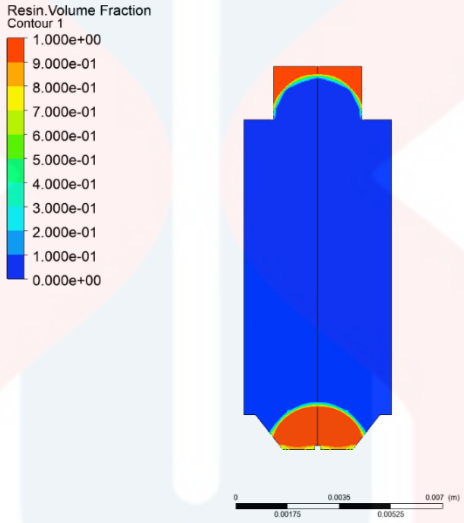

Figure 4.3: Epoxy molding compound simulation results

Table 4.2: Comparison between simulation and experimental

Time (%)	Simulation (Fluent) Viscosity=0.448 Kg/m. s	Experimental
0	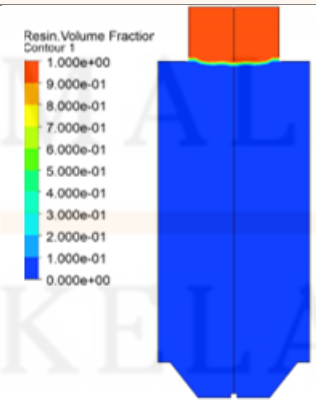	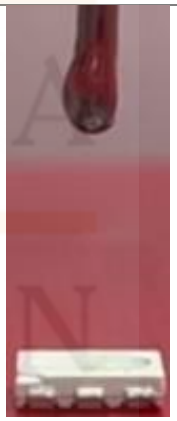

10	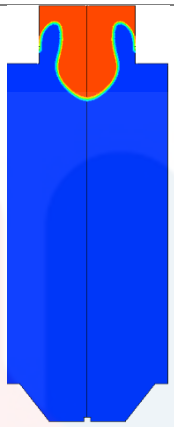	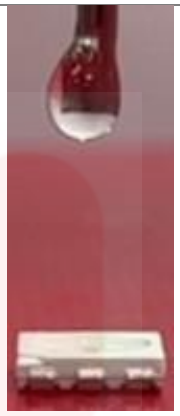
25	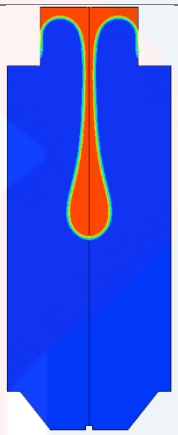	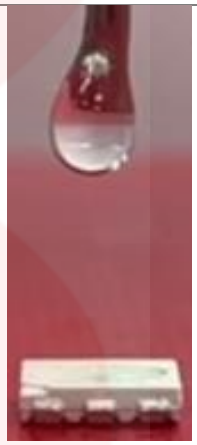
60	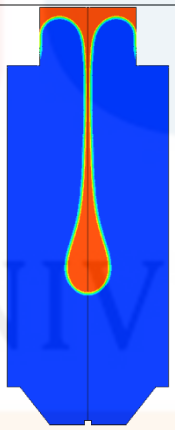	

100	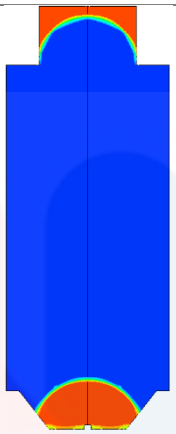	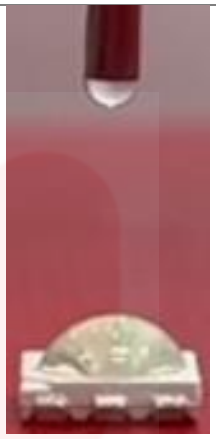

In this simulation, five types of epoxy resins were used which were ERL-4221, EMC, D.E.R.-331, Master Bond EP30-2 and Epotek OG198-54. The parameters and boundary condition in the entire simulation such as inlet speed, contact angle, and injection time were set as constant for the five epoxy resins. Both results from the simulation and experiment are examined and the comparison between structure of the epoxy resins during encapsulation process were illustrated as in Table 4.2. The objective of this simulation was to analyse the effect of five different epoxy resins on the final structure of the encapsulant which leads to the occurrence microvoid that cover the base of the LED which are approximately 2.34mm in diameter. The final structure of the simulation result for the five epoxy resins was expected to be the same as the actual result.

In Table 4.2, EMC was used in the experiment as it has the same viscosity with simulation EMC. From the results, the encapsulation structure for the EMC is the same as the experimental structure and the percentage difference is only 10%. This shows that the simulation setup for the EMC is almost accurate and can be used for the other epoxy materials to compare the final structure of the encapsulant. Based on the results shown in simulation the structure for all five epoxy resins was similar from time duration 0% to 10%. However, starting

from time duration 25% until 100%, the structures for the five epoxy resins started to differ. At the 25%- time duration, ERL-4221 structure has already finish dropping off the epoxy resin while the structure for EMC and Epotek OG198-54 just started to drop off the epoxy resin. D.E.R-331 and Master Bond EP30-2 was faster compared to the other three as at the 25%- time duration, the structure still drops off the epoxy resin completely. At 50%-time duration to 100%-duration which was the final structure, the ERL-4221. EMC, and D.E.R.-331 structure appear like the hemisphere shape as the actual result while for Master Bond EP30-2 and Epotek OG198-54 the structure also fully hemisphere in shape but there has bubble in the simulation until finish running still not disappear. it is considered a high performance resin used in glass-reinforced structural composites, particularly for its outstanding chemical resistance and mechanical properties.(Ham et al., 2012)

From the results obtained, ERL-4221 and D.E.R.-331 tends to have more micro void than three other epoxies. As the material with lower density compared to EMC but for the Master Bond EP30-2 and Epotek OG198-54 with a lower viscosity shorter gel time, it can flow further while liquid form compared to the epoxy with higher viscosity.

4.4 Computational Fluid Dynamics

4.4.1 Effect Microvoid on Different of Epoxy

In this section, the effect microvoid on different of epoxy on LED structure are studied using close up view on LED area. Three parameters are observed which are effect microvoid on different of epoxy materials, effect microvoid on different size of inlet and effect microvoid on different speed of inlet.

Table 4.3: Comparison of microvoids observed among five different epoxy materials

Type of Epoxy	Viscosity (Kg/m. s)	
ERL-4221	0.224	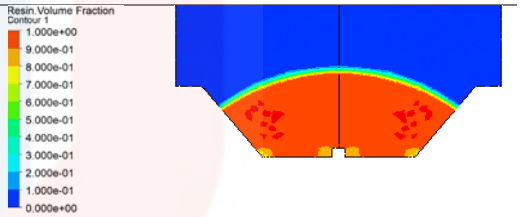
EMC	0.448	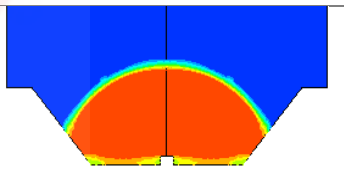
D.E.R.-331	0.896	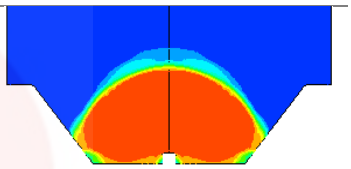
Master Bond EP30-2	0.4	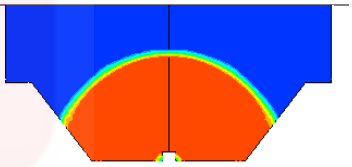
Epotek OG198-54	0.15	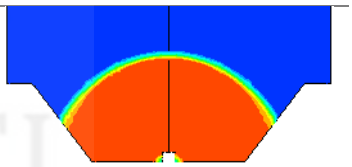

In Table 4.3, which presents the final simulation results for the five epoxy types (ERL-4221, EMC, D.E.R.-331, Master Bond EP30-2, and Epotek OG198-54), it is evident that D.E.R.-331 epoxy exhibits a substantial number of microvoids. These microvoids are not only present on the surface but are also larger in size compared to those observed in other epoxy types. Specifically, D.E.R.-331 epoxy displays numerous microvoids around the LED wall, with four larger microvoid effects on one side of the LED wall and additional effects on the middle of the LED wall.

Epoxy ERL-4221 also demonstrates a microvoid effect, primarily around the LED on the side of the wall, resulting in four microvoid effects. EMC epoxy, on the other hand, shows microvoid effects attributed to the presence of a large layer underneath, resulting in four voids. The size of these microvoids is slightly larger compared to those in ERL-4221 epoxy.

In the case of Epoxy Master Bond EP30-2, only a minor microvoid effect is observed around the small LED in the middle of the LED wall, with two small microvoid effects. Lastly, Epotek OG198-54 epoxy exhibits a microvoid effect similar to Epoxy Master Bond EP30-2, with an effect in the middle of the LED wall, featuring two microvoid effect points. Notably, the left side of the microvoid effect is larger than the right side.

In conclusion, D.E.R.-331 epoxy stands out for having a significant number of microvoid effects, particularly around the LED wall, with four prominent microvoid effects on one side and additional effects in the middle. This distinguishes it from other epoxy types in terms of microvoid formation.

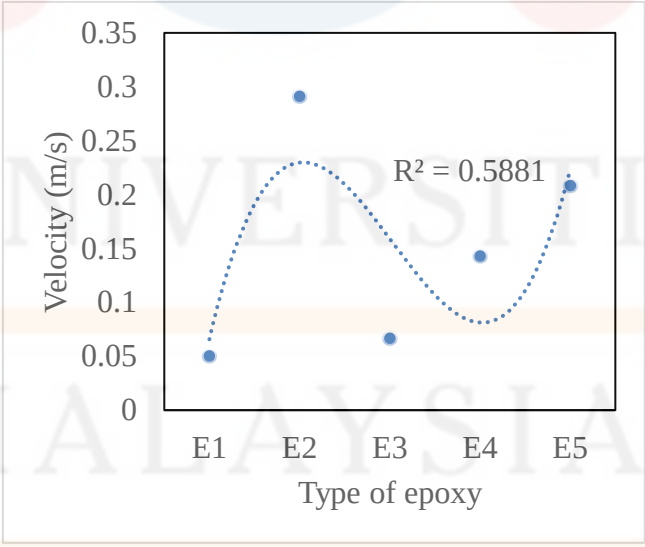

Figure 4.4: Variation in velocity for epoxy

In Figure 4.4, it becomes apparent that the choice of epoxy influences the velocity differently for each epoxy type. For instance, EMC epoxy exhibits the lowest velocity at 0.050312415 m/s. Slightly surpassing EMC epoxy is D.E.R.-331 epoxy, with an increase of 0.016417213 m/s, representing a 4.96% rise, resulting in a velocity of 0.066729628 m/s. The third-highest velocity epoxy is Epotek OG198-54, experiencing an increase of 0.076075812 m/s, corresponding to a 6.53% increment, and yielding a velocity of 0.14280544 m/s. Following this, Master Bond EP30-2 epoxy attains the second-highest velocity at 0.20824364 m/s, marking a 14.07% increase from Epotek OG198-54 epoxy. Finally, ERL-4221 epoxy boasts the highest velocity among the five epoxies, reaching 0.29120737 m/s, with a difference of 0.08296373 m/s from Master Bond EP30-2 epoxy.

Despite the variations in velocity, it can be deduced that the increase in velocity does not directly correlate with the production of microvoids. This conclusion is drawn from the examination of the final results in Table 4.3, which indicates that D.E.R.-331 epoxy, despite having a significant microvoid effect, occupies a middle position in Figure 4.4. This suggests that the velocity alone does not dictate the extent of microvoid production, as observed in the specific characteristics of each epoxy material. Materials with lower melt viscosity and longer gel time have fewer failures.(Kinjo et al., 2022)

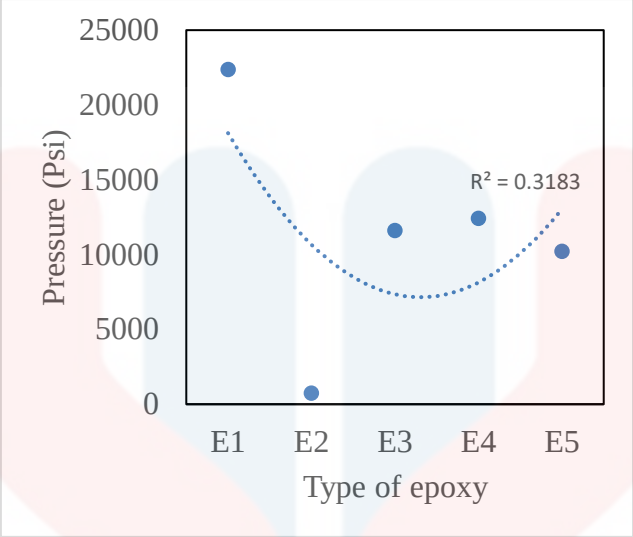

Figure 4.5: Variation in pressure for epoxy

From figure 4.5 it can be observed the effect of different epoxy formulations on the pressure generated. EMC epoxy manifests the highest pressure, registering at 22379.332 pascals. Following closely is Epotek OG198-54 epoxy, occupying the second-highest position with a noteworthy pressure decrease of 9964.996 pascals. This reduction, amounting to 55.47%, results in a pressure reading of 12414.336 pascals. Meanwhile, D.E.R.-331 epoxy exhibits the third-lowest pressure at 11602.357 pascals, experiencing a decrease of 811.979 pascals, equivalent to a 6.54% reduction.

Master Bond EP30-2 epoxy secures the second-lowest position on the pressure scale, recording 10211.516 pascals. Finally, ERL-4221 epoxy demonstrates the lowest pressure among the tested formulations, with a reading of 732.15576 pascals. This marks a considerable decrease of 9479.36024 pascals from Master Bond EP30-2 epoxy, representing a substantial 92.83% reduction.

Correlating these pressure findings with the microvoid effects observed in Table 4.3, it is evident that D.E.R.-331 epoxy exhibits the most pronounced microvoid effect. Interestingly, despite variations in pressure readings across different epoxy formulations, the microvoid

effect in D.E.R.-331 epoxy remains consistent. Notably, the pressure variations observed do not appear to correlate with the extent of microvoid formation. The stability of the microvoid effect in D.E.R.-331 epoxy underlines the notion that extreme pressure conditions do not significantly impact microvoid production, emphasizing the importance of stable pressure conditions in epoxy-based systems. requirements on encapsulating material from reliability aspects are introduced by thoroughly discussing connections between failures in reliability testing and the variables.(Kinjo et al., 2022)

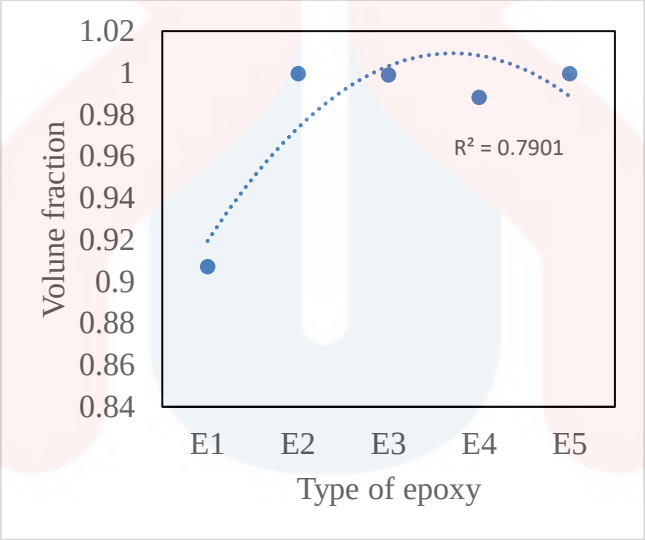

Figure 4.6: Variation in volume fraction for epoxy

Based on the data presented in Figure 4.6, it is evident that EMC epoxy has the lowest volume fraction, measuring 0.90717566, followed by Epotek OG198-54 epoxy with a slightly higher fraction of 0.98819321—an increase of 0.08101755 from EMC. Subsequently, D.E.R.-331 epoxy exhibits a volume fraction of 0.99891996, marking a 1.07% rise from Epotek OG198-54. The second-highest volume fraction is observed in Epoxy Master Bond EP30-2 at 0.99951291, reflecting a marginal increase of 0.0113197. Finally, ERL-4221 epoxy attains the highest volume fraction of 0.99955004, with a negligible percentage difference of 0.004% from

Epoxy Master Bond EP30-2. In summary, the analysis indicates that D.E.R.-331 Epoxy showcases a notable presence of microvoids, especially at the third-highest volume fraction. A very little volume percentage of these nanoparticles can cause a pretty widespread toughening of the epoxy polymer because of their extremely small size and therefore enormous quantity.(Bray et al., 2013)

4.4.2 Effect Microvoid on Different Size of Inlet

In this section, the effect of different size of inlet on microvoid are studied. The same parameters are observed which are microvoid.

Table 4.4: Comparison between five different inlet size

Inlet Size (mm)	
3.2	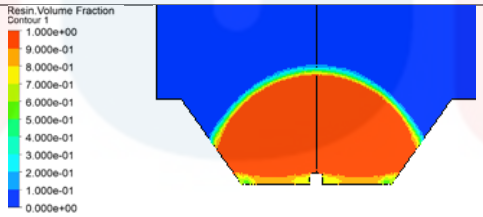
3.4	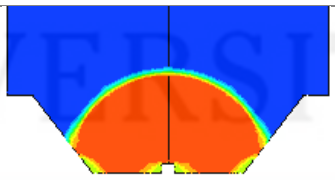
3.6	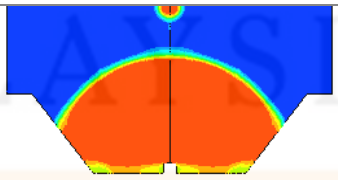

3.8	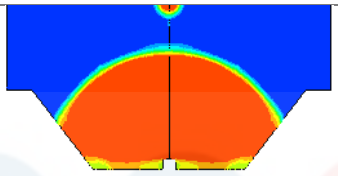
4.0	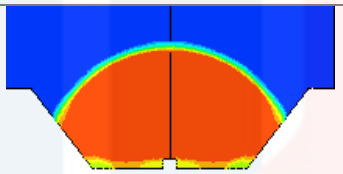

Table 4.4 provides insights into the impact of different inlet sizes on microvoid formation, with five varying sizes considered. A notable observation emerges, indicating that the greatest microvoid effect occurs at the 3.4 mm inlet size. This is evidenced by a substantial cluster of microvoids surrounding the LED wall, featuring as many as four distinct microvoid effects along both the edges and centre of the LED wall. Notably, the largest microvoid effect is observed on the side of the LED wall, contributing to the overall prominence of microvoids. Following closely, the second highest microvoid effect is associated with the 3.6 mm inlet size. In this scenario, microvoid effects are discernible along both the side edge and the middle of the LED wall, resulting in a total of four microvoid effects. Conversely, the third-most prominent microvoid effect is identified at the 3.8 mm inlet size.

This is characterized by two discernible microvoid effects around the LED wall, notably presenting a slightly greenish tint. The 3.2 mm and 3.8 mm inlet sizes share the fourth position in terms of microvoid effects. Upon rough observation, it is noted that the resulting microvoid effects for these inlet sizes are approximately equivalent. Specifically, two microvoid effects manifest around the side of the LED wall. In summation, the analysis suggests that the magnitude of the inlet size does not linearly correlate with an increase in microvoid effects. Contrary to expectations, the 3.4 mm inlet size exhibits the most pronounced microvoid effect compared to other sizes, challenging the assumption that larger inlet sizes would consistently

yield greater microvoid formation. This underscores the complexity of the interplay between inlet size and microvoid effects, emphasizing the need for nuanced considerations in understanding and optimizing these epoxy systems. The encapsulating material is placed into the moulding die pot after being prepared and heated using a high frequency device.(Ham et al., 2012)

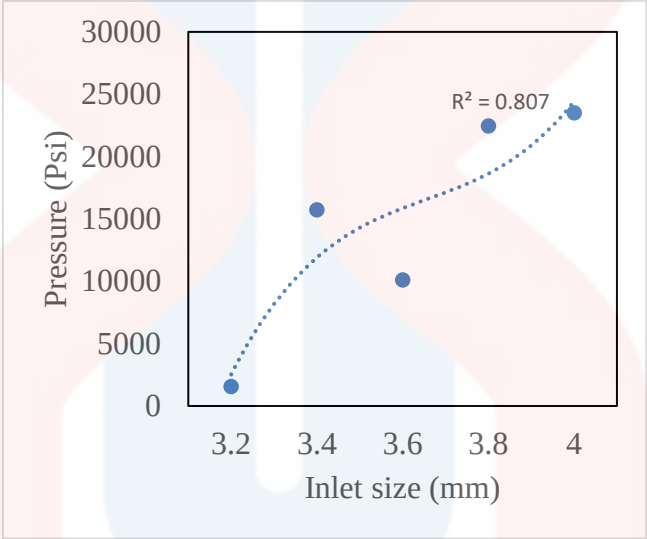

Figure 4.7: Variation in pressure for inlet size

For figure 4.7 it can be observed variations in pressure among the five different inlet sizes. The smallest inlet size, 3.2mm, exhibits the lowest pressure at 1566.6136 pascal. Moving to the slightly larger 3.6mm inlet size, there is a considerable pressure increase to 10113.178 pascals, marking a significant rise of 8546.5644 pascals or an 84.51% increase. The 3.4mm inlet size demonstrates a pressure of 15731.312 pascals, reflecting a 35.71% increase compared to the 3.6mm inlet size. Inlet size 3.8mm follows with a pressure of 22450.289 pascals, indicating a further increase of 6718.977 pascals. The largest pressure is observed at the 3.8mm inlet size, measuring 23498.475 pascals, with a moderate percentage increase of 4.46% from the 3.8mm inlet size. Analysing the simulation results, it can be concluded that the most

consistently distributed pressure occurs at the 3.4mm inlet size. This aligns with the microvoid effect observed in Table 4.4, suggesting that a balanced pressure distribution, rather than the highest pressure, correlates with the most pronounced microvoid effect. Because it is energetically expensive to create new surface, a fluid system will work to reduce surface areas.(Bush & John, 2010)

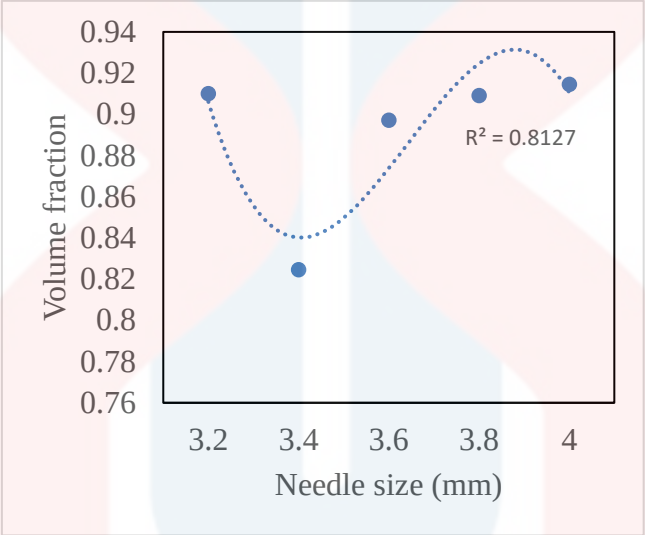

Figure 4.8: Variation in volume fraction for inlet size

For the observation from Figure 4.8 obtained it can be seen that the volume fraction produced remains relatively consistent across four needle sizes, except for needle size 3.4, which displays the lowest volume fraction at 0.82462931. In contrast, the highest volume fraction is associated with needle size 4.0, recording 0.91446024. The disparity between the highest and lowest fractions is 0.08983093, representing a substantial percentage difference of 90.18%. The volume fractions for needle sizes 3.2mm, 3.6mm, and 3.8mm fall in between, with 3.2mm exhibiting a volume fraction of 0.91000682. However, for 3.6mm, a slight decrease is observed at 0.89715725, indicating a reduction of 0.01284957. On the other hand, needle size 3.8mm experiences a subsequent increase, reaching a volume fraction of 0.90900546, with a percentage increase of 1.30%. In summary, the findings suggest that the

volume fraction generated by each needle size doesn't necessarily follow a linear increase as the needle size increases. Notably, needle size 3.4, which yields the lowest volume fraction, corresponds with the observations in Table 4.4, indicating that lower volume fractions can contribute to the production of a higher number of microvoids compared to instances with higher volume fractions. This underscores the nuanced relationship between needle size, volume fraction, and the resultant microvoid effects. One of the most thorough investigations on how adding microcapsules to epoxy matrices affects them found that as the percentage of microcapsules increased, so did the elastic modulus and ultimate stress.(Kanellopoulos et al., 2016)

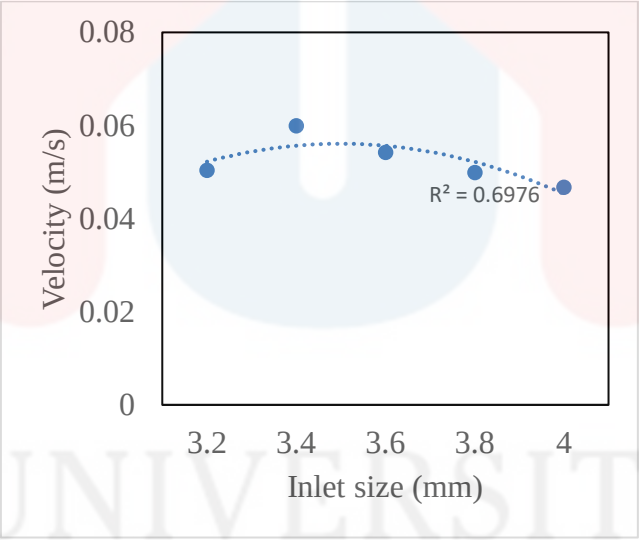

Figure 4.9: Variation in velocity for inlet size

For the observation of from Figure 4.9, which illustrates the velocities corresponding to five different inlet sizes, reveals notable patterns. The highest velocity is observed at inlet size 3.4 mm, registering at 0.059886057 m/s. Following closely, the second-highest velocity is recorded at inlet size 3.6 mm, measuring 0.054210369 m/s. The difference between these two velocities is 0.005675688 m/s. The third-highest velocity is associated with inlet size 3.2 mm, indicating a velocity of 0.050337814 m/s. The percentage difference between the second and

third velocities is 7.14%. Moving to the lower velocities, inlet size 3.8 mm exhibits a velocity of 0.049860615 m/s, with a difference of 0.004477754 m/s compared to the inlet size 3.2 mm. Finally, the lowest velocity is observed at inlet size 4.0 mm, measuring 0.04670351 m/s, with a difference of 0.003157105 m/s from the velocity at inlet size 3.8 mm. In conclusion, the data from Figure 4.9 indicates that higher velocities are associated with larger microvoid effects, as evidenced by Table 4.4. Inlet size 3.4 mm, which exhibits a substantial microvoid effect, corresponds with the highest velocity. While inlet size 3.6 mm follows closely, the relationship between velocity and microvoid effects becomes apparent. Additionally, the viscosity of the epoxy is noted as a potential factor influencing microvoid occurrence, further emphasizing the intricate interplay of factors contributing to the observed effects. Compared to the reactive oligomers, the particle size and volume fraction of the second phase may be more readily regulated.(Kanellopoulos et al., 2016)

4.4.3 Effect Microvoid on Different Speed of Inlet

In this section, the effect microvoid on different speed of inlet. The parameter is observed which are the microvoid that happen when five different speeds been use for simulation and how it effects the microvoid.

Table 4.5: Comparison between five different speeds of inlet

Inlet speed (m/s)	
0.34	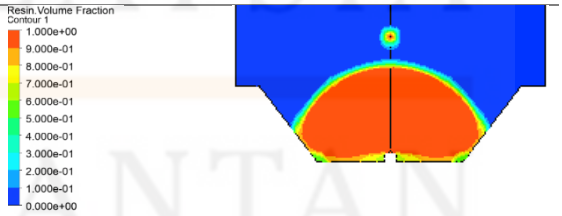

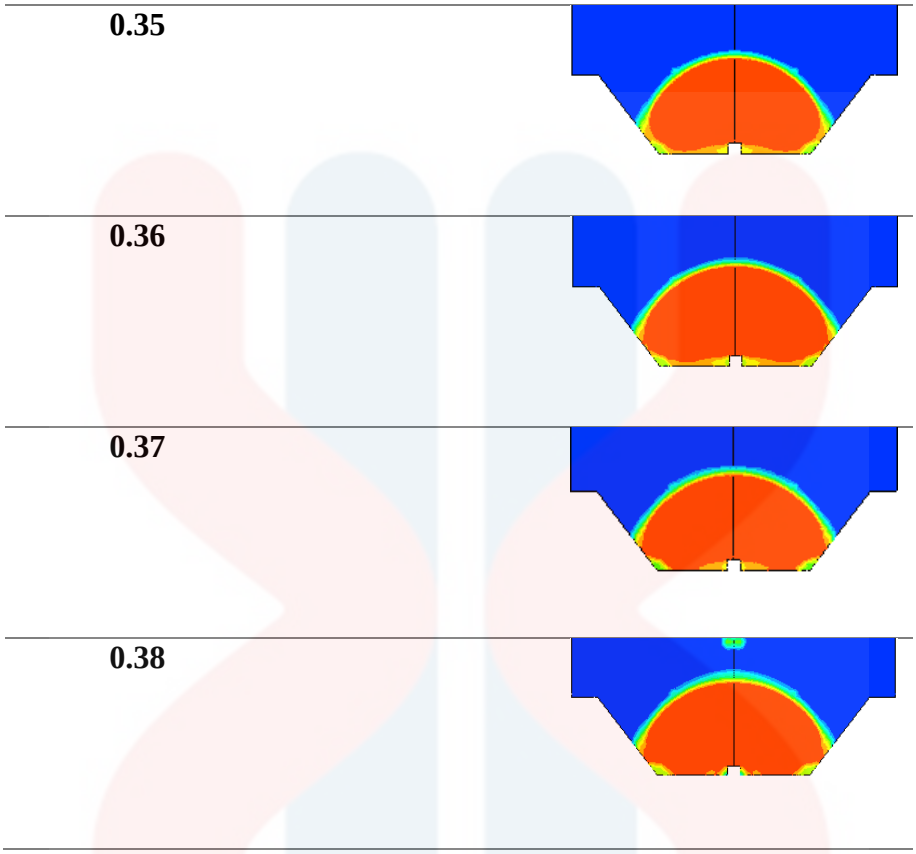

From Table 4.5 shows that there are five different types of inlet speed used to see the microvoid effect. By observation it can be made that the inlet speed that has the most effect of microvoid is at 0.38 because it has a green patch which is the most microvoid compared to the others as many as four microvoid patches which are also the largest from the others. The second most noticeable from the simulation results is the inlet speed 0.36 because of the microvoid patches on the side edges of the LED wall and in the middle of the LED wall. For the next one, the inlet speed is 0.34 because it is more or less the same as the microvoid effect at the inlet speed of 0.36, but the resulting microvoid effect is smaller. The next smallest is the inlet speed 0.35 because it has a microvoid effect on the side of the LED wall, it shows a slightly smaller effect than before but in the middle of the LED wall it does not show a microvoid effect and finally the least microvoid effect is on the inlet speed 0.37 because it is smaller from an inlet speed of 0.35 with the resulting microvoid effect being almost undetectable. The conclusion is

that this simulation shows that the fastest inlet speed has the biggest microvoid effect on the epoxy, but it happens at a speed of 0.38 not below because it is not necessarily faster the more microvoid effect that results maybe it depends on other factors.

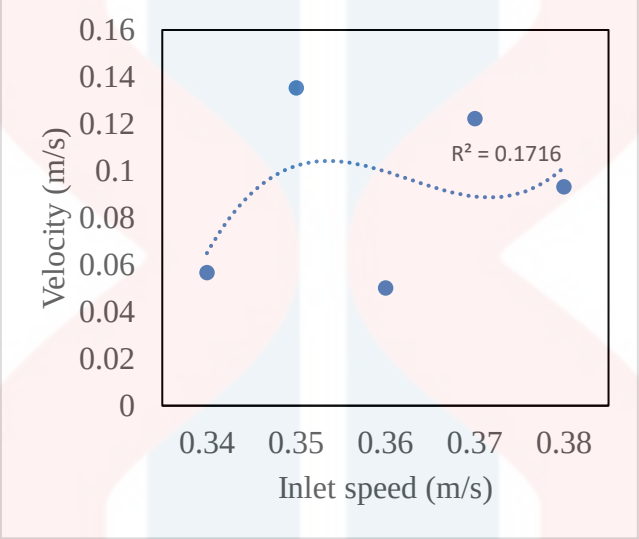

Figure 4.10: Variation in velocity for inlet speed

In Figure 4.10 shows the velocity graph with the difference in inlet speed used can be seen at the inlet speed 0.34 (m/s) which is 0.056667008 (m/s) it happens to have the second lowest velocity compared to the inlet speed 0.36 (m/s) which the lowest inlet speed is 0.050123107 (m/s) it can be said that the velocity difference between these two is as much as 0.006543901 (m/s) with a percentage of only 11.55%. the slightly higher of these two inlet speeds is 0.38 (m/s) with the difference between these two being 0.043077077 (m/s) with the velocity value being 0.093200184 (m/s). next is the second highest velocity is inlet speed 0.37 (m/s) with a value of 0.12218009 (m/s) it is higher with the drop rate difference between inlet speed 0.38 (m/s) and 0.37 (m/s) is 23.72%. lastly for the most velocity is at inlet speed 0.35 (m/s) with the velocity value is 0.13524503 (m/s) with the difference between the two highest

of 0.01306494 (m/s). The conclusion that can be made from the observation from Figure 4.8 that the effect of many microvoids does not result from the high velocity but with a stable velocity only the one in the middle which is at the inlet speed 0.38 is proven in Table 4.5 which shows the most microvoids at this speed. sufficiently tiny enough that when resin transfer moulding manufacturing procedures are used, they are not filtered out of the matrix by the fibre preforms when introduced to the matrices for fiber-reinforced composite materials.(Bray et al., 2013)

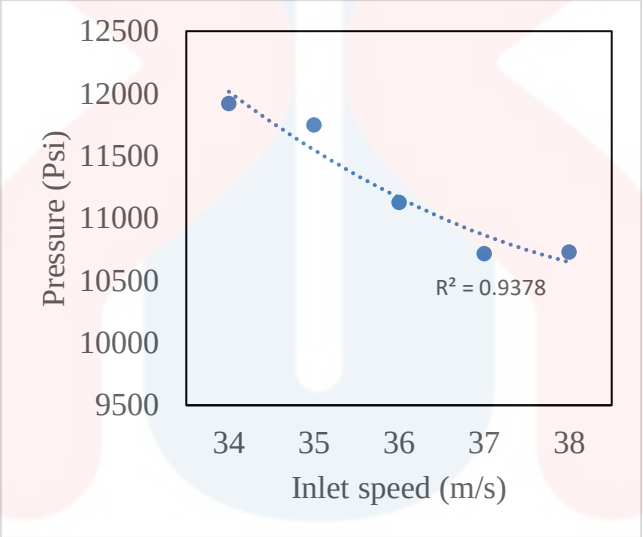

Figure 4.11: Variation in pressure for inlet speed

Figure 4.11 shows the results from the simulation, showing that the pressure data used is reasonably even; that is, it decreases at each inlet speed when the speed is increased, but not at the inlet speed of 0.38 (m/s), which does not show the same pressure decrease trend. It can be seen that the highest pressure is at inlet speed 0.34 (m/s) with a pressure of 11921.623 pascal and decreases at inlet speed 0.35 by 173.136 pascal, which is 11748.487. It shows that it continues to decrease at speed 0.36 (m/s) with more, which is 621.671, with the decreasing percentage for this inlet speed is 5.29%, which means the pressure is 11126.816 pascal. For the

next inlet speed, which is the inlet speed 0.37 (m/s) also, less pressure is given to it, which is 10715.927 pascal with a decrease of 410.889 pascal. Inlet speed 0.38 (m/s) shows an increase of 0.13%. This shows that the pressure does not necessarily increase with the inlet speed, so the pressure decreases with This evidence also shows that there is a pressure difference; this is evidence against Table 4.5 that the inlet speed 0.38 (m/s) has more microvoid effects compared to the others and does not become high and lowest pressure factors cause the microvoid effect to occur a lot because inlet speed 0.38 (m/s) is the second lowest. The adequately mixed solution was put in a sealed mold to guarantee solvent retention. The mold was sealed using vacuum bagging and sticky tape such that no air or gap occurred between the solution and seal to avoid solvent evaporation during cure.(Campbell, 2010)

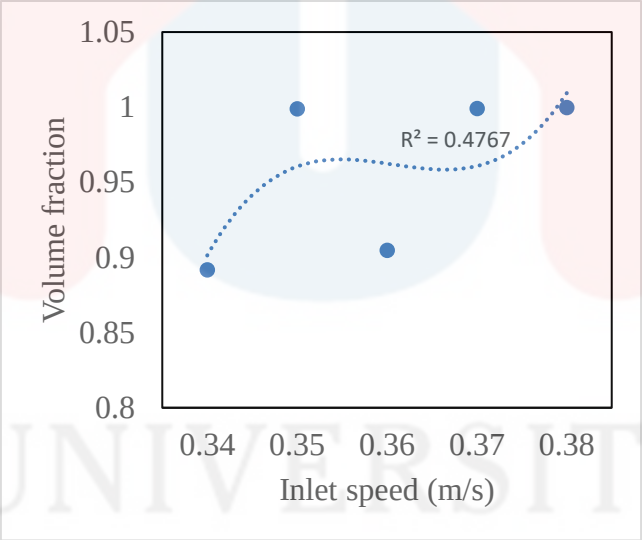

Figure 4.12: Variation in volume fraction for inlet speed

In figure 4.12 showing the variation of volume fraction in five different inlet speeds, it can be observed that the highest volume fraction is inlet speed 0.38 (m/s) which is 0.99976093 with the second highest being at inlet speed 0.37 (m/s) which is 0.99922657 with a slight difference of 0.00053436. the next third highest is the inlet speed of 0.35 (m/s) which is

0.99893695 with a percentage difference of only 0.02%. The second lowest is at the inlet size 0.36 (m/s) it is 0.90480876 with the difference between the third and fourth is 0.09412819. lastly for the lowest which is inlet speed 0.34 (m/s) it is 0.89171147 with the fourth percentage difference with the lowest volume fraction is 1.45%. the conclusion that can be made from this data is that for the inlet speed of 0.38 (m/s) it has a lot of microvoid effect with the highest volume fraction but for the second most effect which is the inlet speed of 0.36 (m/s) it can be said to sit in the middle , then this can only see the content of the volume fraction only not a factor to see the effects related to the microvoid effect. the curing reactions and the release of the curing heat may cause localized overheating in the cavity, which may in turn result in a high warpage and even cracking and/or delamination in the encapsulants upon cooling.(Liu et al., 2004)

CHAPTER 5

CONCLUSION AND FUTURE RECOMMENDATIONS

5.1 Conclusion

In conclusion, the present study has yielded promising results in the investigation of the impact of microvoid on LED encapsulation, incorporating three distinct parameters. Notably, one of these parameters, selected for validation in the simulation, demonstrated a commendable 90% similarity to the experimental results, with a marginal discrepancy of only 10%. This consistency underscores the reliability of the simulation in capturing the effects under consideration.

Delving into the manipulation of viscosity and concentrations, the research revealed divergent outcomes in relation to the microvoid effect, particularly concerning the initial parameter. The second parameter, pertaining to the area of epoxy inclusion, mirrored the significant impact observed in the first parameter, albeit with variations limited to the area of inclusion. Noteworthy is the constancy maintained across the five simulations, where settings remained unaltered, accentuating the robustness of the findings.

The exploration of the third parameter, involving different insert speeds, underscored distinct effects on microvoid production in epoxy. The variability in outcomes among the five simulations, each employing different speeds, accentuates the nuanced influence of insert speeds on microvoid effects.

In summary, among the three parameters examined, the most pronounced microvoid effect was discerned in the parameter associated with the variance in size of the epoxy insert. This parameter exhibited consistent microvoid effects across all scenarios, emphasizing its significance in influencing microvoid production. Furthermore, an analysis of the three

parameters, namely difference in pressure, volume fraction, and velocity, revealed a lack of discernible distinctions in their impact on the observed increase in microvoids.

This study contributes valuable insights that can guide future research endeavors. By shedding light on the nuanced interplay of parameters influencing microvoid effects in LED encapsulation, this investigation lays the groundwork for further exploration and refinement of encapsulation processes.

5.2 Recommendation

In light of the findings presented in this thesis, a valuable suggestion for future research endeavors is to expand the scope of the study. A broader investigation would not only enhance exposure for new students but also contribute to a more comprehensive understanding of the subject matter. Moreover, it is recommended that the design of the simulation model be upgraded from the current 2-dimensional representation to a more sophisticated 3-dimensional drawing mode.

The adoption of a 3-dimensional design offers the potential for a more realistic portrayal of the encapsulation process, closely aligning with the actual experimental conditions. Although the present study utilized a 2-dimensional approach due to time constraints, transitioning to a 3-dimensional model holds the promise of yielding more captivating and nuanced results. Specifically, the incorporation of a 3-dimensional design could render the epoxy production process at the inlet, as it descends onto the LED, more compelling. While acknowledging that such an adjustment may prolong the duration required to obtain final results, the enhanced realism and increased granularity of outcomes make it a worthwhile investment.

Furthermore, a 3-dimensional design allows for a more comprehensive visualization of the experimental outcomes, offering a broader perspective compared to the limitations inherent

in a 2-dimensional representation. By embracing this advanced modeling approach, the study could potentially unveil additional insights and complexities inherent in the microvoid effects on LED encapsulation.

In conclusion, the recommendation arising from this simulation study is to transition from a 2-dimensional to a 3-dimensional design for future investigations. This adjustment is anticipated to enrich the final results, providing a more in-depth and realistic depiction of the encapsulation process. It is hoped that this thesis serves as a valuable contribution, both in terms of its current findings and as a catalyst for further advancements in the field of LED encapsulation research.

REFERENCES

Anderson, J. D. (1992). Governing Equations of Fluid Dynamics. *Computational Fluid Dynamics*, 15–51. https://doi.org/10.1007/978-3-662-11350-9_2

Andrade, B., Song, Z., Li, J., Zimmerman, S. C., Cheng, J., Moore, J. S., Harris, K., & Katz, J. S. (2015). New frontiers for encapsulation in the chemical industry. *ACS Applied Materials and Interfaces*, *7*(12), 6359–6368. https://doi.org/10.1021/acsami.5b00484

Bray, D. J., Dittanet, P., Guild, F. J., Kinloch, A. J., Masania, K., Pearson, R. A., & Taylor, A. C. (2013). The modelling of the toughening of epoxy polymers via silica nanoparticles: The effects of volume fraction and particle size. *Polymer*, *54*(26), 7022–7032. https://doi.org/10.1016/j.polymer.2013.10.034

Bush, & John. (2010). Definition and Scaling of Surface Tension. *Creative Commons BY-NC-SA*, 4–11. https://ocw.mit.edu/

Campbell, D. G. (2010). *by*. *December*.

Çevik, B., Ozçatalbaş, Y., & Gülenç, B. (2016). Rührreibschweißen einer 7075-T651-Aluminiumlegierung. *Praktische Metallographie/Practical Metallography*, *53*(1), 6–23. https://doi.org/10.3139/147.110363

Chen, Z., Liu, Y., & Sun, H. (2021). Physics-informed learning of governing equations from scarce data. *Nature Communications*, *12*(1), 1–13. https://doi.org/10.1038/s41467-021-26434-1

EP30-2 Product Information | MasterBond.com. (n.d.). Retrieved December 12, 2023, from https://www.masterbond.com/tds/ep30-2

EPO-TEK ® OG198-54. (n.d.). Retrieved December 13, 2023, from www.epotek.com

Ham, H. A. Q. P., Chemical, D., Arks, M. A. J. M., & Chemical, D. (2012). *Epoxy Resins*.

https://doi.org/10.1002/14356007.a09

High-Power LED Encapsulation Inspection – Electronics | Cognex. (n.d.). Retrieved May 23, 2023, from https://www.cognex.com/en-my/industries/electronics/led-manufacturing/high-power-led-encapsulation-inspection

Huang, J. C., Chu, Y. P., Wei, M., & Deanin, R. D. (2004). Comparison of epoxy resins for applications in light-emitting diodes. *Advances in Polymer Technology*, *23*(4), 298–306. https://doi.org/10.1002/adv.20018

Huang, Y., & Kinloch, A. J. (1992). The toughness of epoxy polymers containing microvoids. *Polymer*, *33*(6), 1330–1332. https://doi.org/10.1016/0032-3861(92)90785-U

Kanellopoulos, A., Giannaros, P., & Al-Tabbaa, A. (2016). The effect of varying volume fraction of microcapsules on fresh, mechanical and self-healing properties of mortars. *Construction and Building Materials*, *122*, 577–593. https://doi.org/10.1016/j.conbuildmat.2016.06.119

Kinjo, N., Ogata, M., Nishi, K., & Kaneda, A. (2022). Epoxy Molding Compounds as Encapsulation Materials for Microelectronic Devices. *Speciality Polymers / Polymer Physics*, 1–48. https://doi.org/10.1515/9783112484647-002

Ley 25.632. (2002). *済無No Title No Title No Title*. *April*.

Liu, S. L., Chen, G., & Yong, M. S. (2004). EMC characterization and process study for electronics packaging. *Thin Solid Films*, *462–463*(SPEC. ISS.), 454–458. https://doi.org/10.1016/j.tsf.2004.05.080

Roslan, H., Abdul Aziz, M. S., Abdullah, M. Z., Kamarudin, R., Ishak, M. H. H., Ismail, F., & Irawan, A. P. (2020). Analysis of LED wire bonding during encapsulation process. *IOP Conference Series: Materials Science and Engineering*, *1007*(1). https://doi.org/10.1088/1757-899X/1007/1/012173

Shin-Etsu Silicone : Silicone Materials for LEDs. (n.d.). Retrieved May 23, 2023, from

https://www.shinetsusilicone-global.com/products/usage/led/index.shtml

Silicone Encapsulation – TIC Industries. (n.d.). Retrieved May 23, 2023, from https://tic-industries.com/products/silicone-encapsulation/

Visualization, G. (2020). *Computational Fluid Dynamics for Propulsion Technology : Final Report*.

Zissis, G., Bertoldi, P., Serrenho, T. (2018). *Update on the Status of LED-Lighting world market since 2018, EUR 30500 EN, Publications Office of the European Union, Luxembourg, 2021, ISBN 978-92-76-27244-1, doi:10.2760/759859, JRC122760*. https://doi.org/10.2760/759859